JOURNAL OF THEORETICAL AND APPLIED MECHANICS
53, 4, pp. 859-872, Warsaw 2015
DOI: 10.15632/jtam-pl.53.4.859

A STUDY ON LOW VELOCITY IMPACT RESPONSE OF FGM RECTANGULAR PLATES WITH 3D ELASTICITY BASED GRADED FINITE ELEMENT MODELING

Kamran Asemi

Department of Mechanical Engineering, Tehran North Branch, Islamic Azad University, Tehran, Iran

Sattar Jedari Salami

Department of Mechanical Engineering, Damavand Branch, Islamic Azad University, Damavand, Iran

e-mail: sattar.salami@damavandiau.ac.ir

Low velocity impact behavior of rectangular plates made of functionally graded materials (FGMs) based on three-dimensional theory of elasticity is studied in this paper. The modified Hertz contact law, which is appropriate for graded materials, is employed. On the basis of the principle of minimum potential energy and the Rayleigh Ritz method, the graded finite element modeling is applied. Solution of the nonlinear resulted system of equations in the time domain is accomplished via an iterative numerical procedure based each time on Newmark's integration method. The effects of various involved parameters, such as the graded property profile, projectile velocity and projectile density on time histories of contact force, lateral deflection and normal stresses are investigated in detail. To present efficiency of the present work, several numerical examples are included. The main novelty of the present research, which has not been reported in literature, is considering the difference of lateral deflection through the thickness of the FGM plate due to analyzing three-dimensional elasticity of the plate.

Keywords: low velocity impact, functionally graded plate, three dimensional elasticity, graded finite element

1. Introduction

Functionally graded materials yield as a category of novel composite materials in which mechanical properties vary in one, two or even three specific direction(s). FGMs are mainly composed of metal and ceramic components. Unlike the traditional composites, which are piecewise homogeneous mixtures or layered structures, material properties of FGMs are affected by those of all constituent materials, so that mechanical properties of the FGMs can be monitored to vary continuously throughout the structure. Advantages of FGMs over laminated composites are the elimination of the delamination mode of failure, reduction thermal stresses, residual stresses and stress concentration factors.

Low velocity impact response of solid structures is a conventional topic in structural mechanics. There are various approaches to model the contact between the projectile and target. Spring mass models, energy balance technique and a direct approach are the commonly utilized methods. A complete survey of these approaches with their defects or advantages may be found in a book by Abrate (1998).

A wide range of studies has been carried out on dynamic analysis of FGM structures which mostly used the plate and shell theories (Asemi *et al.*, 2010; Qian *et al.*, 2004; Sun and Luo, 2011; Behjat *et al.*, 2009; Kiani *et al.*, 2012; Noda *et al.*, 2012; Derras *et al.*, 2013; Ghannad and Nejad, 2013; Yaghoobi and Torabi, 2013). For thin plates, the classical plate theory (CPT) is used to analyze FG plates. Due to neglecting the effect of shear deformation through the thickness of

FG plates, the application of this theory to moderately thick or thick plate structures can lead to considerable errors. Therefore, for eliminating the lack of CPT for moderately thick and thick FG plates, the first, third and higher shear deformation theories and also the 3D elasticity solutions, some modifications are done to include the effects of transverse shear deformation. Among these analyses, 3D elasticity analysis of plates not only provides accurate results but also allows further physical insights, which cannot otherwise be estimated by the other two dimensional or plate theory analyses.

A literature review on the subject of FGM structures under low velocity impact as a dynamic analysis discloses that researches on this topic are rare in the open literature. There are a class of works dealing with the simulation of low velocity impact response of FGMs using the commercial software. For instance, Gunes and Aydin (2010) modeled the three dimensional response of FGM media using the commercial finite element software. In that research an FGM circular plate was divided into a number of layers in the thickness direction, where each one was supposed as an isotropic homogeneous layer. Gunes *et al.* (2011) developed their previous work for the case of elasto-plastic impact response of circular FGM plates. Mori-Tanaka scheme was applied to obtain the equivalent properties of each single layer. For the case of a sandwich beam with FGM core, Etemadi *et al.* (2009) extended a three dimensional simulation on the low velocity impact response of the structure.

To achieve the low velocity impact response of FGM plates, Larson and Palazotto (2009) and Larson *et al.* (2009) developed a combined experimental, computational and analytical method. In those investigations, a property estimation sequence was introduced for specifying the local elastic properties of a two-phased, two constituent FGM plate subjected to impact loading. Numerical simulations and experimental tests were carried out on Ti-TiB FGM plates. The evaluated results were then used to accomplish a finite element model of the problem. It was indicated that the low-velocity impact response of the plate based on FEM results were in good agreement with those obtained experimentally. To date, a few works have been studied on dynamic behavior of plates made of functionally graded materials in two directions. Wirowski (2009) studied free vibrations of thin annular plates made of a functionally graded material that is made of a two-phase functionally graded composite. The plate has a periodically inhomogeneous microstructure slowly varying along a circular coordinate, but smoothly graded properties in the radial direction. Also, Wirowski (2011, 2012) analyzed the free vibration response of a thin rectangular plate band made of a nonlinear functionally graded material. The material properties varied periodically in one direction and non-linearly in the other one. The effect of the material distribution on the overall response of the composite was studied. As might be concluded, a very strong dependency of frequency of free vibrations of the plate band on the material distribution was observed for the bracket and very weak for the simple support on both sides.

There are only a few investigations related to the mathematical formulation of low velocity impact in FGMs. The main reason may be the contact force modeling between the projectile and target. Giannakopoulos and Suresh (1997) studied the indentation of solids into a graded half-space. Two types of grading profiles, i.e. the exponential distribution and polynomial type of dispersion were considered in their works. In addition, the two-dimensional contact was also studied by Giannakopoulos and Pallot (2000). Those investigations may be useful to deduce the contact-force expression for graded materials. For example, Mao *et al.* (2011) analyzed the response of a shallow spherical shell under the low velocity impact in a thermal field. Properties of the FGM media were distributed across the thickness based on an exponential function. The immovable case of clamped edges was considered and the resulted equations were solved via the Galerkin method. The developed contact force formulation for the exponential property distribution revealed that the force-indentation relation in exponential FGMs was similar to the Hertz contact force, where force is proportional to $\alpha^{3/2}$. The contact stiffness, however, was related to geometrical and material parameters of contacting structures, impacting a sphere and

an FGM shallow spherical shell. For media with transversely isotropic characteristics, Conway (1956) and Turner (1980) concluded a force-indentation relation through the Hertz contact force expression. In those researches, also only the contact stiffness was influenced by a property variation of the structure and again, force was proportional to $\alpha^{3/2}$.

Such a character motivates the investigators to modify the Hertz contact force of finite thickness media in a way to account the graded profile through the thickness. For instance, Larson and Palazotto (2006) developed a Hertzian type of the contact force in which the contact stiffness was modified to account the grading profile. The impact response of a circular FGM plate was analyzed in their work. Shariyat and Jafari (2013) obtained the low velocity impact behavior of a circular plate with both radial and transverse graded profiles. In their work, symmetrical motion equations were obtained based on the first order shear deformation plate theory and the results were found via the Galerkin method. In another study, Shariyat and Farzan (2013) investigated the response of an FGM plate in rectangular shape under the eccentric impact. In that research, the first order shear deformation beam theory was used and the effect of in--plane loads was also taken into consideration. Khalili *et al.* (2013) studied the response of a thin FGM plate in rectangular shape that was subjected to low velocity impact. However in that research, in-plane inertia effects were neglected. With the introduction of Airy stress function, the in-plane motion equations were replaced by the compatibility equation. Besides, a linear contact force model was employed in which the contact force varied linearly with respect to indentation. The contact stiffness was obtained based on the mass-spring model and the results were compared with the ABAQUS software. In another study, Dai *et al.* (2012) studied the low velocity impact behaviour of shear deformable FGM circular plates. In that investigation, also the contact formulation of Giannakopoulos and Suresh (1997) was implemented. The solution in space and time domains was obtained based on the orthogonal collocation point method and Newmark's method, respectively.

According to the above literature review, to date, the equivalent single-layer theories have been applied to analyze the low velocity impact response of FGM plates. Due to difficulty in obtaining solutions for low velocity impact analysis of FGM plates based on 3D elasticity, solutions are available only through a number of problems by the use of plate theories. Therefore, powerful numerical methods are needed to solve the governing equations. The graded finite element method (GFEM) is a relatively new numerical technique in structural analysis. Kim and Paulino (2002), and Zhang and Paulino (2007), developed a GFEM approach for modeling nonhomogeneous structures. In their studies, it was shown that the conventional FE formulations cause a discontinuous stress field in the direction perpendicular to the material property gradation, while the graded elements gave a continuous and smooth variation. Also, Asemi *et al.* (2012) studied the dynamic response of thick short length FGM cylinders under an internal impact loading using the graded finite element method. Ashrafi *et al.* (2013) presented a comparative study between the graded finite element and boundary element formulations capable of modeling nonhomogeneous behavior of FGM structures. They showed that using the conventional finite element modeling such that the material property is constant within an element for dynamic problems leads to considerable discontinuities and inaccuracies. On the other, hand by using the graded finite element method in which the material property is graded continuously through the elements, the accuracy of results can be improved without increasing the mesh size.

To the best knowledge of the authors, there are no accessible documents in literature on involving effects of the material inhomogeneity of the FGM plates based on the graded elements and three dimensional elasticity theory on low velocity impact response of FGM plates. So, the present study aims at developing a numerical approach for low velocity impact of FGM rectangular plates based on the three-dimensional theory of elasticity. The governing equations are derived based on the principle of minimum potential energy and the Rayleigh Ritz method. In this regard, variations of the material properties are interpolated using general shape functions.

An iterative numerical procedure in the space domain is used which is suitable for an arbitrary case of boundary conditions. This style accompanied with Newmark's method is employed to solve the nonlinear resulted field equations. The modified contact force model of Larson and Palazotto (2006), which considered the property variations through the thickness, is utilized. The influences of various involved parameters such as projectile velocity, power law index, projectile mass on time histories of the contact force and lateral deflection of the target are studied in detail.

2. The governing equations

2.1. Description of variations of the material properties

A functionally graded rectangular plate whose length, width, and thickness are marked by a, b, and h, respectively, is considered as it is shown in Fig. 1. The top surface of the plate is made of pure metal and the bottom surface of pure ceramic. The material properties of the plate vary continuously through the thickness direction according to a power law distribution

$$P = P_c + (P_m - P_c)\Big(\frac{z}{h}\Big)^n \tag{2.1}$$

where P is material property such as elasticity modulus and mass density. n is the non-negative volume fraction index and the z coordinate is measured from the bottom surface of the plate. The subscripts c and m are referred to a ceramic and metal, respectively.

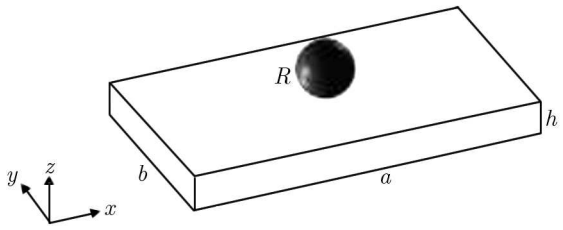

Fig. 1. Geometry of the plate and the impactor

2.2. The effective stiffness of the contact region

Integrating the local volume fraction of the constituent material of the top layer leads to the total volume fraction of the mentioned material

$$V_m = \frac{1}{h}\int_0^h \Big(\frac{z}{h}\Big)^n dz = \frac{1}{1+n} \qquad V_c = 1 - V_m \tag{2.2}$$

Therefore, the apparent material properties of the FGM plate at the impact region can be expressed as

$$\begin{aligned} &E_z = \Big(\frac{V_c}{E_{z_c}} + \frac{V_m}{E_{z_m}}\Big)^{-1} \qquad G_{xz} = G_{yz} = \Big(\frac{V_c}{G_c} + \frac{V_m}{G_m}\Big)^{-1} \\ &E_x = E_y = E_c V_c + E_m V_m \qquad \rho = \rho_c V_c + \rho_m V_m \end{aligned} \tag{2.3}$$

where G is the shear modulus of the material.

Based on the investigation carried out by Olsson (1992), the impact load applied by a spherical projectile may be related to the indentation value of an isotropic half space through the following Hertz-type relation

$$F(\alpha) = K_h \alpha^{3/2} \tag{2.4}$$

where α is the indentation value, and the impact stiffness is

$$K_h = \frac{4}{3} Q_\alpha \sqrt{R} \tag{2.5}$$

where R is the indenter nose radius, and Q_α is defined as

$$\frac{1}{Q_\alpha} = \frac{1}{Q_{zi}} + \frac{1}{Q_{zp}} \qquad Q_{zk} = \frac{E_{zk}}{1-\nu_{zk}^2} \qquad k = i, p \tag{2.6}$$

where E_{zk} is the elastic modulus in the transverse direction and ν_{zk} is Poisson's ratio of the plate (p) or impactor (i). For the case in which the rigidity of the impactor is much more than that of the impacted half space, Eq. (2.6) may be reduced to

$$Q_\alpha = Q_{zp} \tag{2.7}$$

It is evident that the impact force and the indentation value are considerably smaller when the same indenter impacts a very thin plate instead of a half space. For this reason, Swanson (2005) modified Eq. (2.4) in the following form for a transversely isotropic plate with a finite thickness

$$F(\alpha) = \beta K_h \alpha^{3/2} \tag{2.8}$$

where β is an empirical correction factor that tends to unity for thickness to indentation ratios exceeding three. On the other hand, Turner (1980) proved that the apparent modulus of a plate that incorporates influences of the transverse variations of material properties at the impact region may be determined as follows

$$Q_\alpha = \frac{2}{\alpha_1 \alpha_3} \tag{2.9}$$

where

$$\begin{aligned} &\alpha_1 = \sqrt{\frac{1}{1-\nu_{xy}^2}}\Big(\frac{E_x}{E_z} - \nu_{xz}^2\Big) \qquad \alpha_2 = \frac{1}{1-\nu_{xy}^2}\Big[\frac{E_x}{2G_{xz}} - \nu_{xz}(1+\nu_{xy})\Big] \\ &\alpha_3 = \sqrt{\frac{\alpha_1+\alpha_2}{2}}\Big(\frac{1-\nu_{xy}}{G_{xy}}\Big) \end{aligned} \tag{2.10}$$

2.3. Equations of motion of an FGM plate

In absence of the body forces, the equations of motion for an FGM rectangular plate can be written as follows

$$\sigma_{ij,j} = \rho(z)\ddot{u}_i \tag{2.11}$$

where $i, j = x, y, z$, and the comma denotes partial differentiation with respect to Cartesian coordinate variables. Hence, $u_x = u$, $u_y = v$, $u_z = w$ are displacement components along the x, y and z axes, respectively. Also, ρ is mass density which depends on the z coordinate, and σ_{ij} are the stress components.

2.4. Stress-strain relations

The constitutive relation based on the three- dimensional theory of elasticity is as follows

$$\boldsymbol{\sigma} = \mathbf{D}\boldsymbol{\varepsilon}$$

$$\mathbf{D} = \frac{E(z)(1-\nu)}{(1+\nu)(1-2\nu)} \begin{bmatrix} 1 & \frac{\nu}{1-\nu} & \frac{\nu}{1-\nu} & 0 & 0 & 0 \\ \frac{\nu}{1-\nu} & 1 & \frac{\nu}{1-\nu} & 0 & 0 & 0 \\ \frac{\nu}{1-\nu} & \frac{\nu}{1-\nu} & 1 & 0 & 0 & 0 \\ 0 & 0 & 0 & \frac{1-2\nu}{2(1-\nu)} & 0 & 0 \\ 0 & 0 & 0 & 0 & \frac{1-2\nu}{2(1-\nu)} & 0 \\ 0 & 0 & 0 & 0 & 0 & \frac{1-2\nu}{2(1-\nu)} \end{bmatrix} = E(z)\boldsymbol{\Lambda} \tag{2.12}$$

where $\mathbf{D}$ is the elastic coefficients matrix. It is assumed that the elasticity modulus E varies in the z direction while Poisson's ratio ν is constant. The constant part of the matrix $\mathbf{D}$ is defined as $\mathbf{\Lambda}$.

2.5. Strain-displacement relations

The strain displacement relations of the infinitesimal theory of elasticity in the rectangular Cartesian coordinates are

$$\varepsilon_{ij} = \frac{1}{2}(u_{i,j} + u_{j,i}) \tag{2.13}$$

Strain-displacement relations (2.13) may be written as

$$\boldsymbol{\varepsilon} = \mathbf{dq} \qquad \mathbf{d} = \begin{bmatrix} \frac{\partial}{\partial x} & 0 & 0 \\ 0 & \frac{\partial}{\partial y} & 0 \\ 0 & 0 & \frac{\partial}{\partial z} \\ \frac{1}{2}\frac{\partial}{\partial y} & \frac{1}{2}\frac{\partial}{\partial x} & 0 \\ 0 & \frac{1}{2}\frac{\partial}{\partial z} & \frac{1}{2}\frac{\partial}{\partial y} \\ \frac{1}{2}\frac{\partial}{\partial z} & 0 & \frac{1}{2}\frac{\partial}{\partial x} \end{bmatrix} \qquad \mathbf{q} = \begin{bmatrix} u \\ v \\ w \end{bmatrix} \tag{2.14}$$

2.6. Boundary and initial conditions

For a simply supported plate, the essential boundary conditions are defined as

$$\begin{aligned} &w(0,y,z) = w(a,y,z) = w(x,0,z) = w(x,b,z) = 0 \\ &v(0,y,z) = v(a,y,z) = u(x,0,z) = u(x,b,z) = 0 \end{aligned} \tag{2.15}$$

And initial conditions for the system of equations are as follows

$$\mathbf{q}_0 = \dot{\mathbf{q}}_0 = 0 \qquad \alpha_0 = 0 \qquad \dot{\alpha}_0 = V_0 \tag{2.16}$$

3. Graded finite element modeling

The three-dimensional 8-node linear brick element is considered. In contrast to the conventional solid (brick) elements, material properties are interpolated using the shape functions. Following the common FE approximation, the displacement components vector $\mathbf{q}$ of an arbitrary point of the element may be related to the nodal displacement vectors of the element $\boldsymbol{\delta}^{(e)}$ through the shape function matrix $\mathbf{N}$, as

$$\begin{aligned} &\mathbf{q}(\xi,\eta,\zeta) = \mathbf{N}(\xi,\eta,\zeta)\boldsymbol{\delta}^{(e)} \qquad \boldsymbol{\delta}^{(e)} = \begin{Bmatrix} U_1 & V_1 & W_1 & \dots & U_8 & V_8 & W_8 \end{Bmatrix}^{\mathrm{T}} \\ &\mathbf{N} = \begin{bmatrix} N_1 & 0 & 0 & N_2 & 0 & 0 & N_3 & 0 & 0 & N_4 & 0 & 0 & N_5 & 0 & 0 & N_6 & 0 & 0 & N_7 & 0 & 0 & N_8 & 0 & 0 \\ 0 & N_1 & 0 & 0 & N_2 & 0 & 0 & N_3 & 0 & 0 & N_4 & 0 & 0 & N_5 & 0 & 0 & N_6 & 0 & 0 & N_7 & 0 & 0 & N_8 & 0 \\ 0 & 0 & N_1 & 0 & 0 & N_2 & 0 & 0 & N_3 & 0 & 0 & N_4 & 0 & 0 & N_5 & 0 & 0 & N_6 & 0 & 0 & N_7 & 0 & 0 & N_8 \end{bmatrix} \end{aligned} \tag{3.1}$$

The components of the shape matrix may be expressed in terms of the natural coordinates (Zienkiewicz and Taylor, 2005)

$$N_i(\xi,\eta,\zeta) = \frac{1}{8}(1+\xi_i\xi)(1+\eta_i\eta)(1+\zeta_i\zeta) \tag{3.2}$$

where $-1 \leqslant \xi \leqslant 1$, $-1 \leqslant \eta \leqslant 1$ and $-1 \leqslant \zeta \leqslant 1$.

In addition to the displacement field, the heterogeneity of the material properties of the FGM may also be determined based on their nodal values. Therefore, a graded finite element method (GFEM) may be used to effectively trace smooth variations of the material properties at the element level. Using GFEM for the modeling of gradation of the material properties leads to more accurate results than dividing the solution domain into homogenous elements. In this regard, the shape functions similar to those of the displacement field may be used

$$E=\sum_{i=1}^{8}E_iN_i=\mathbf{N}\boldsymbol{\Xi}\qquad\qquad \rho=\sum_{i=1}^{8}\rho_iN_i=\mathbf{N}\boldsymbol{\mathcal{R}} \tag{3.3}$$

where E_i and ρ_i are the modulus of elasticity and mass density corresponding to node i. $\mathbf{N}$, $\boldsymbol{\Xi}$ and $\boldsymbol{\mathcal{R}}$ are vectors of shape functions, modulus of elasticity and mass densities of each element, and they are as

$$\mathbf{N}=[N_1,\ldots,N_8]_{1\times 8}\qquad\qquad \boldsymbol{\Xi}=[E_1,\ldots,E_8]^{\mathrm{T}}_{1\times 8}\qquad\qquad \boldsymbol{\mathcal{R}}=[\rho_1,\ldots,\rho_8]^{\mathrm{T}}_{1\times 8} \tag{3.4}$$

Therefore, Eq. (2.12) may be rewritten as

$$\mathbf{D}=\boldsymbol{\Lambda}\mathbf{N}\boldsymbol{\Xi} \tag{3.5}$$

Substituting (3.1) into (2.14) gives the strain matrix of the element (e) as

$$\boldsymbol{\varepsilon}^{(e)}=\mathbf{d}\mathbf{N}^{(e)}\boldsymbol{\delta}^{(e)}=\mathbf{B}\boldsymbol{\delta}^{(e)} \tag{3.6}$$

The governing equations of the FE model may be derived based on the principle of minimum potential energy and the Rayleigh Ritz method. The total potential energy of the plate may be expressed as

$$\begin{aligned}\Pi^{(e)}=&\frac{1}{2}\int\limits_{V^{(e)}}(\boldsymbol{\varepsilon}^{(e)})^{\mathrm{T}}\boldsymbol{\sigma}^{(e)}\,dV-\int\limits_{A^{(e)}}\mathbf{q}^{\mathrm{T}}\mathbf{p}\,dA+\int\limits_{V^{(e)}}\boldsymbol{\rho}\mathbf{q}^{\mathrm{T}}\ddot{\mathbf{q}}^{(e)}\,dV\\&+m_pw_p\ddot{w}_p-\frac{2}{5}K_h\Big[w_p-W\Big(\frac{a}{2},\frac{b}{2},h\Big)\Big]^{\frac{5}{2}}\end{aligned} \tag{3.7}$$

where $W(a/2,b/2,h)$ is nodal transverse displacement of the contact node, m_p and w_p are the mass and displacement value of the impactor.

By employing (3.5) and (3.6) in (3.7), the following equation could be derived

$$\begin{aligned}\Pi^{(e)}=&\frac{1}{2}\int\limits_{V^{(e)}}(\boldsymbol{\delta}^{(e)})^{\mathrm{T}}\mathrm{B}^{\mathrm{T}}\boldsymbol{\Lambda}\mathbf{N}\boldsymbol{\Xi}\mathbf{B}\boldsymbol{\delta}^{(e)}\,dV-\int\limits_{A^{(e)}}(\boldsymbol{\delta}^{(e)})^{\mathrm{T}}\mathbf{N}^{\mathrm{T}}\mathbf{p}\,dA\\&+\int\limits_{V^{(e)}}\mathbf{N}\boldsymbol{\mathcal{R}}(\boldsymbol{\delta}^{(e)})^{\mathrm{T}}\mathbf{N}^{\mathrm{T}}\mathbf{N}\ddot{\boldsymbol{\delta}}^{(e)}\,dV+m_pw_p\ddot{w}_p-\frac{2}{5}K_h\Big[w_p-W\Big(\frac{a}{2},\frac{b}{2},h\Big)\Big]^{\frac{5}{2}}\end{aligned} \tag{3.8}$$

where $V^{(e)}$ and $A^{(e)}$ are respectively the volume and area of the element, $\mathbf{p}$ is the traction vector and the two last terms of Eq. (3.8) represent the work of inertial loads.

Therefore, employing the principle of minimum total potential energy leads to the following result

$$\begin{aligned}\frac{\partial\Pi^{(e)}}{\partial(\boldsymbol{\delta}^{(e)})^{\mathrm{T}}}=0\Rightarrow&\left(\int\limits_{V^{(e)}}\mathbf{N}\boldsymbol{\mathcal{R}}\mathbf{N}^{\mathrm{T}}\mathbf{N}\,dV\right)\ddot{\boldsymbol{\delta}}^{(e)}+\left(\int\limits_{V^{(e)}}\mathbf{B}^{\mathrm{T}}\boldsymbol{\Lambda}\mathbf{N}\boldsymbol{\Xi}\mathbf{B}\,dV\right)\boldsymbol{\delta}^{(e)}\\&-\int\limits_{A^{(e)}}\mathbf{N}^{\mathrm{T}}\mathbf{p}\,dA+K_h\Big[w_p-W\Big(\frac{a}{2},\frac{b}{2},h\Big)\Big]^{\frac{3}{2}}=0\end{aligned} \tag{3.9}$$

Equation (3.9) for each element of the FGM plate may be written in a compact form as

$$\mathbf{M}^{(e)}\ddot{\boldsymbol{\delta}}^{(e)} + \mathbf{K}^{(e)}\boldsymbol{\delta}^{(e)} = \mathbf{F}^{(e)} \tag{3.10}$$

where

$$\begin{aligned} \mathbf{K}^{(e)} &= \int\limits_{V^{(e)}} \mathbf{B}^{\mathrm{T}}\boldsymbol{\Lambda}\mathbf{N}\boldsymbol{\Xi}\mathbf{B}\, dV \qquad \mathbf{M}^{(e)} = \int\limits_{V^{(e)}} \mathbf{N}\boldsymbol{\mathcal{R}}\mathbf{N}^{\mathrm{T}}\mathbf{N}\, dV \\ \mathbf{F}^{(e)} &= \int\limits_{A^{(e)}} \mathbf{N}^{\mathrm{T}}\mathbf{p}\, dA - K_h\Big[w_p - W\Big(\frac{a}{2},\frac{b}{2},h\Big)\Big]^{\frac{3}{2}} \end{aligned} \tag{3.11}$$

It should be noted that the contact force should be set equal to zero after separation of the impactor from the plate.

Also by minimizing the total potential energy with respect to the displacement of the impactor, we have

$$\frac{\partial \Pi^{(e)}}{\partial w_p} = 0 \Rightarrow m_p\ddot{w}_p - K_h\Big[w_p - W\Big(\frac{a}{2},\frac{b}{2},h\Big)\Big]^{\frac{3}{2}} \tag{3.12}$$

On the other hand, the governing equation of the impactor is as follows

$$F(\alpha) = -m_p\ddot{w}_p = K_h\alpha^{\frac{3}{2}} \tag{3.13}$$

Based on the deformation kinematics

$$\alpha = w_p - W\Big(\frac{a}{2},\frac{b}{2},h\Big) \tag{3.14}$$

Equation (3.12) may be rewritten as

$$\ddot{W}\Big(\frac{a}{2},\frac{b}{2},h\Big) = -\frac{K_h}{m_p}\alpha^{\frac{3}{2}} - \ddot{\alpha} \tag{3.15}$$

Now, by assembling the element matrices, the global dynamic equilibrium equations for the FGM plate can be obtained as

$$\mathbf{M}\ddot{\boldsymbol{\delta}} + \mathbf{K}\boldsymbol{\delta} = \mathbf{F} \tag{3.16}$$

Various numerical methods can be employed to solve Eq. (3.16) in the space and time domains. The Newmark direct integration algorithm (Zienkiewicz 2005) is used to discretize the system of ordinary differential Eq. (3.16) in time domain. With the given initial conditions shown in Eq. (2.16), Eq. (3.15) and Eq. (3.16) have to be solved simultaneously. However, since the system of equations is nonlinear, the Newton-Raphson technique has to be used in each time step to reach a convergent solution. For each time step, the iteration lasts until the difference between the previous two iterative steps is smaller than 0.1%.

4. Results and discussion

4.1. Verification of the results

To validate the current work, the low velocity impact response of a homogenous plate is considered. So the geometry and material properties of the plate are considered as: $a = 0.2\,\mathrm{m}$,

$b = 0.1\,\mathrm{m}$, $E = 70\,\mathrm{GPa}$, $\rho = 2707\,\mathrm{kg/m^3}$, and for the rigid spherical impactor: $R = 15\,\mathrm{mm}$, $V_0 = 1\,\mathrm{m/s}$.

Due to inaccessibility to experimental results, the empirical constant β of Swanson's equation (Eq. (2.8)) is presumed unity in the present analysis (Turner, 1980). The calculated time histories of the contact force and mid-plane deflection ($x = a/2$, $y = b/2$, $z = h/2$) for the simply supported FGM rectangular plate is compared with the numerical results obtained by commercial FEM software ANSYS Workbench as shown in Fig. 2. In order to model the problem in ANSYS Workbench, $25 \times 25 \times 4$ brick elements through the x, y and z directions are utilized. The frictionless type of contact between surfaces of the projectile and plate is used. The results are in good agreement with those obtained from software simulation. The differences are probably due to using a real contact in ANSYS Workbench and modified Hertz contact law in the present research.

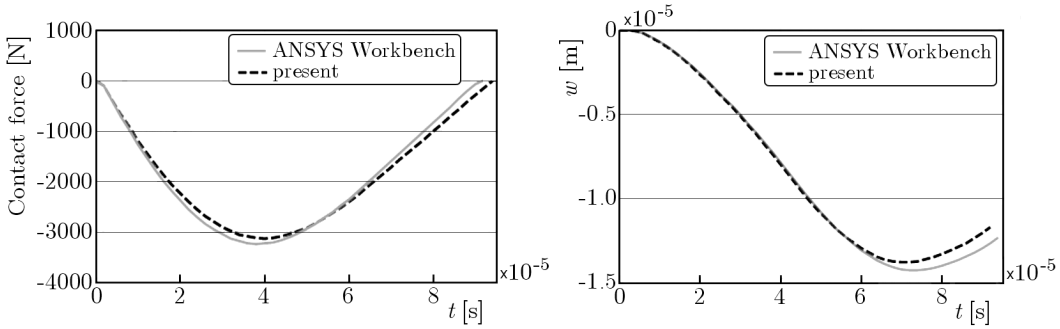

Fig. 2. Time history of the contact force and mid-plane deflection of the plate compared with ANSYS Workbench

4.2. Evaluation of effects of different parameters on the low velocity impact responses of the FGM plate

In this Section, an effective analysis is employed based on various parameters. The FGM rectangular plate and a rigid spherical impactor are specified as the following: $a = 200\,\mathrm{mm}$, $b = 100\,\mathrm{mm}$, $h = 20\,\mathrm{mm}$, $R_i = 15\,\mathrm{mm}$, $\rho_i = 7800$, 8900, 9850 and $11300\,\mathrm{kg/m}s$, $V_0 = 1$, 2, 3, $4\,\mathrm{m/s}$, $E_m = 70\,\mathrm{GPa}$, $\rho_m = 2707\,\mathrm{kg/m^3}$, $E_c = 380\,\mathrm{GPa}$, $\rho_c = 3800\,\mathrm{kg/m^3}$, $\nu = 0.3$.

The effects of the volume fraction index on the time histories of the contact force, projectile velocity, mid-plane ($x = a/2$, $y = b/2$, $z = h/2$) deflection of the plate, top displacement ($x = a/2$, $y = b/2$, $z = h$) of the plate, and normal stress components of the mid-plane are shown in Figs. 3-5, respectively, for $n = 1, 3, 5$. The results are obtained for $V_0 = 1\,\mathrm{m/s}$ and $m_p = 110\,\mathrm{gr}$, ($\rho_i = 7800\,\mathrm{kg/m^3}$). According to Fig. 3a, it may be observed that since the volume fraction index of the material properties increases, the volume fraction of the ceramic part and the stiffness of the FGM plate increases so that the peak contact force is increased and, as a result of this, the contact time duration is decreased. Figure 3b indicates that whatever the material property index of FGM plate is increased, the departure velocity of projectile is elevated. This result reveals that by increasing the stiffness of the FGM plate, the stored energy in the plate is reduced. Furthermore, as illustrated in Fig. 3b, the higher index case yields a more rapid velocity reduction compared with the lower one, because the FGM plate is strengthened by an increase in the index of material property.

On the other hand, according to Fig. 4a increasing the volume fraction index and, consequently, enhancing the stiffness of the plate leads to a decrease in the deflection of the plate. As a result of this occurrence, the curvature of the plate decreases and the in-plane normal stress component σ_{yy} is reduced, see Fig. 5a. The observed result for peel stress σ_{zz} is vague. That is probably affected by the material nonlinearity of the FGM plate, see Fig. 5b. Also Figs. 4a

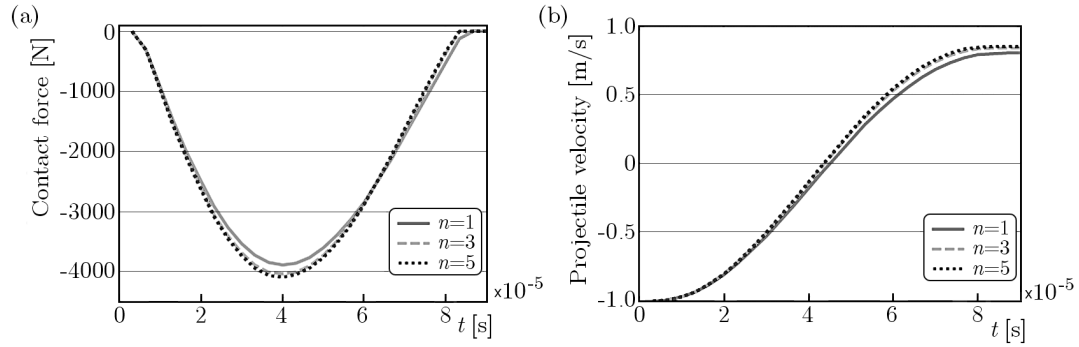

Fig. 3. A comparison among time histories of the contact force (a) and of the projectile velocities (b) for different volume fraction indices

and 4b illustrate that the top displacement of the FGM plate is greater than the mid-plane one, because the FGM plate is analyzed by three dimensional theory of elasticity, therefore, the lateral compressibility of the plate is considered. The mentioned result has not been reported due to using Equivalent Single Layer (ESL) theories in such works in the literature.

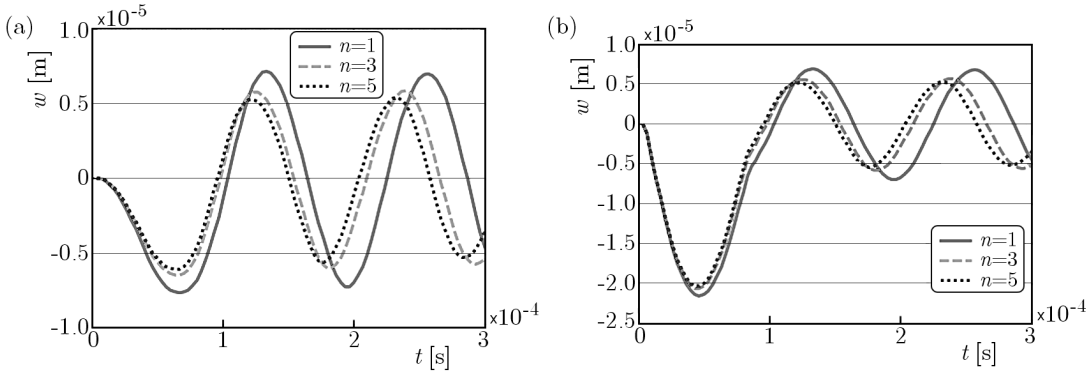

Fig. 4. A comparison among time histories of the mid-plane deflections (a) and of the top displacement (b) for different volume fraction indices

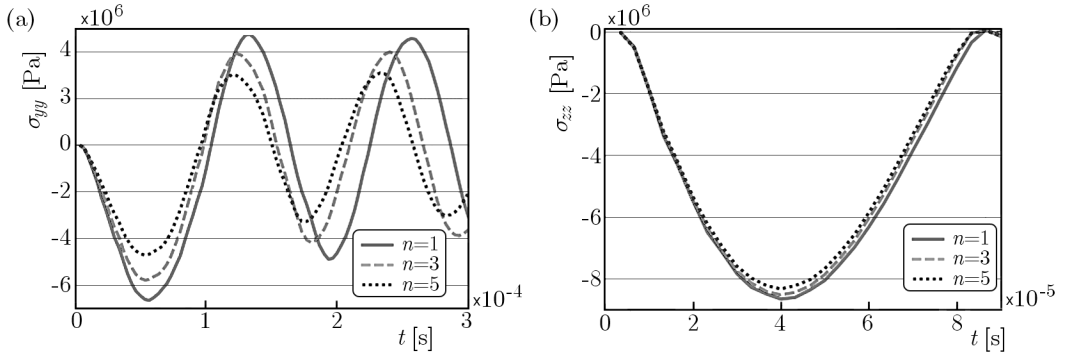

Fig. 5. A comparison among time histories of the in-plane stress σ_{yy} (a) and of the peel stress σ_{zz} (b) for different volume fraction indices

The effects of the initial velocity of the projectile on the contact force, mid-plane deflection of the plate and departure velocity of the projectile are depicted in Figs. 6a,b and 7, respectively ($n = 1$, $m_p = 110\,\mathrm{gr}$). It may be concluded that increasing the initial velocity of the projectile causes enhancement of the peak contact force. However, the high initial velocity of projectile decreases the contact time duration. Figure 7 reveals how the departure velocity may vary as the initial velocity of the projectile increases. According to this result, the ratio of the departure to the initial velocity of the projectile is decreased by increasing the initial velocity of the projectile. This is because that by increasing the initial velocity, the stored energy in the plate is increased. On the other hand, whatever the initial velocity of projectile is increased, the velocity during the contact time is reduced more rapidly.

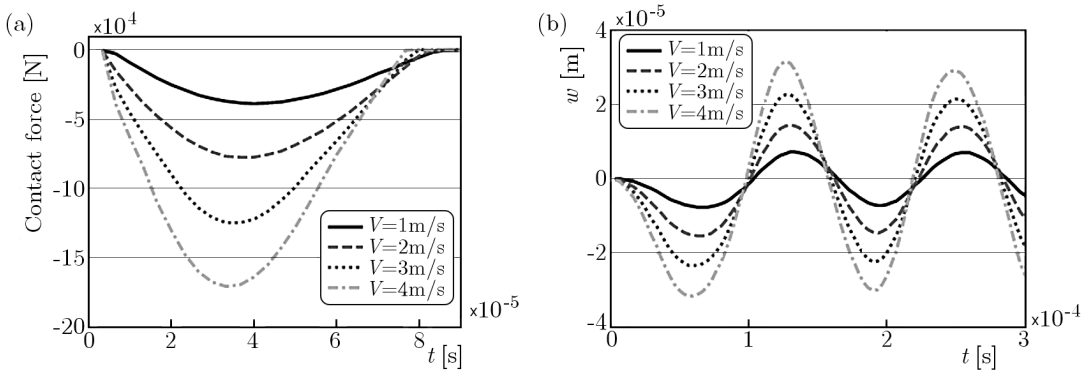

Fig. 6. Influence of the initial velocity of the projectile on the time history of the contact force (a) and of the lateral deflection of the plate (b); $n = 1$

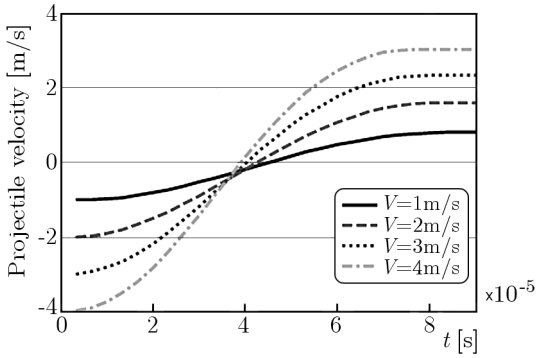

Fig. 7. Influence of the initial velocity of the projectile on the departure velocity of the projectile; $n = 1$

The effects of the projectile mass on the contact force and mid-plane lateral deflection of the plate for the simply supported FGM plate are presented in Figs. 8a and 8b, respectively for $n = 1$ and $V_0 = 1\,\mathrm{m/s}$. As it may be deduced from Fig. 8a, an increase in the projectile mass increases the peak contact force due to increasing the impact energy. Also, it elevates the contact time duration, and this result is in contrast with the effect of initial velocity of the projectile. It is because the increase in the mass of projectile highlights the inertia effect. As it may be observed in Fig. 8b, an increase in the projectile mass reduces the deflection wave propagation because this increase raises the contact duration time. Also, by increasing the projectile mass, the maximum deflection is enhanced.

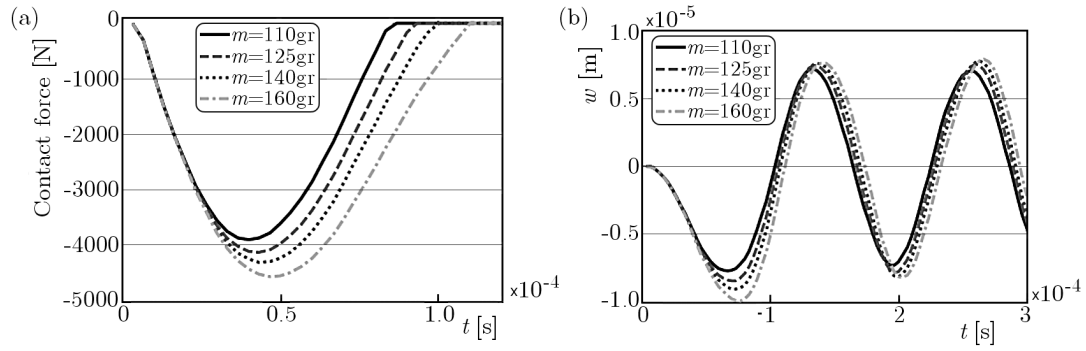

Fig. 8. Effect of the projectile mass on the time history of the contact force (a) and of the lateral deflection of plate (b); $n = 1$

5. Conclusion

In this research, a numerical approach for the low-velocity impact of FGM plates based on the three-dimensional theory of elasticity is extended. By applying the three-dimensional graded elements for analysis of the plates, discontinuities of the stress distribution that are present in the conventional FE results, are eliminated. The influence of the volume fraction index of the FGM plate, initial velocity of the projectile and projectile mass on the parameters such as time histories of the contact force, velocity of the projectile, lateral deflection and normal stresses are studied. The main novelty of the present research which has not been reported in literature is the consideration of the difference of lateral deflection through the thickness of the FGM plate due to analysis of three-dimensional elasticity of the plate.

References

1. Abrate S., 1998, *Impact on Composite Structures*, Cambridge University Press
2. Asemi K., Salehi M., Akhlaghi M., 2010, Dynamic analysis of functionaly graded thick truncated cone, *International Journal of Mechanics and Materials in Design*, **6**, 367-378
3. Asemi K., Akhlaghi M., Salehi M., 2012, Dynamic analysis of thick short FGM cylinders, *Meccanica*, **47**, 1441-1453
4. Ashrafi H., Asemi K., Shariyat M., Salehi M., 2013, Two-dimensional modeling of heterogeneous structures using graded finite element and boundary element methods, *Meccanica*, **48**,663-680
5. Behjat B., Salehi M., Sadighi M., Armin A., Abbasi M., 2009, Static, dynamic and free vibration analysis of functionally graded piezoelectric panels using finite element method, *Journal of Intelligent Materials Systems and Structures*, **20**, 1635-1646
6. Conway H.D., 1956, Analytical model for delamination growth during small mass impact on plates, *ZAMP*, **7**, 80-85
7. Dai H.L., Guo Z.Y., Yang L., 2012, Nonlinear dynamic response of functionally graded materials circular plates subject to low-velocity impact, *Journal of Composite Materials*, DOI: 10.1177/0021998312458132
8. Derras M., Kaci A., Draiche K., Tounsi A., 2013, Non-linear analysis of functionally graded plates in cylindrical bending based on a new refined shear deformation theory, *Journal of Theoretical and Applied Mechanics*, 51, 339-348
9. Etemadi E., Afaghi Khatibi A., Takaffoli M., 2009, 3D finite element simulation of sandwich panels with a functionally graded core subjected to low velocity impact, *Composite Structures*, **89**, 28-34

10. Ghannad M., Nejad M.Z., 2013, Elastic solution of pressurized clamped-clamped thick cylindrical shells made of functionally graded materials, *Journal of Theoretical and Applied Mechanics*, **51**, 1067-1079

11. Giannakopoulos A.E., Suresh S., 1997, Indentation of solids with gradients in elastic properties: part I. Point force, *International Journal of Solids and Structures*, **34**, 2357-2392

12. Giannakopoulos A.E., Pallot P., 2000, Two-dimensional contact analysis of elastic graded materials, *Journal of Mechanics and Physics of Solids*, **48**, 1597-1631

13. Gunes R., Aydin M., 2010, Elastic response of functionally graded circular plates under a drop--weight, *Composite Structures*, **92**, 2445-2456

14. Gunes R., Aydin M., Apalak M.K., Reddy J.N., 2011, The elasto-plastic impact analysis of functionally graded circular plates under low-velocities, *Composite Structures*, **93**, 860-869

15. Khalili S.M.R., Malekzadeh K., Veysi Gorgabad A., 2013, Low velocity transverse impact response of functionally graded plates with temperature dependent properties, *Composite Structures*, **96**, 64-74.

16. Kiani Y., Shakeri M., Eslami M.R., 2012, Thermoelastic free vibration and dynamic behaviour of an FGM doubly curved panel via the analytical hybrid Laplace-Fourier transformation, *Acta Mechanica*, **223**, 1199-1218

17. Kim J.H., Paulino G.H., 2002, Isoparametric graded finite elements for nonhomogeneous isotropic and orthotropic materials, *Journal of Applied Mechanics*, **69**, 502-514

18. Larson R.A., Palazotto A., 2006, Low velocity impact analysis of functionally graded circular plates, *Proceedings of IMECE2006 2006 ASME International Mechanical Engineering Congress and Exposition*, Chicago, Illinois, USA, paper No.: IMECE2006-14003

19. Larson R.A., Palazotto A.N., 2009, Property estimation in FGM plates subjected to low--velocity impact loading, *Journal of Mechanics of Materials and Structures*, **4**, 1429-1451

20. Larson R.A., Palazotto A.N., Gardenier H.E., 2009, Impact Response of titanium and titanium boride monolithic and functionally graded composite plates, *AIAA Journal*, **47**, 676-691

21. Mao Y.Q., Fu Y.M., Chen C.P., Li Y.L., 2011, Nonlinear dynamic response for functionally graded shallow spherical shell under low velocity impact in thermal environment, *Applied Mathematical Modelling*, **35**, 2887- 2900

22. Noda N., Ootao Y., Tanigawa Y., 2012, Transient thermoelastic analysis for a functionally graded circular disk with piecewise power law, *Journal of Theoretical and Applied Mechanics*, **50**, 831-839

23. Olsson R., 1992, Impact response of orthotropic composite plates predicted from a one-parameter differential equation, *AIAA Journal*, **30**, 1587-1596.

24. Qian L.F., Batra R.C., Chen L.M., 2004, Static and dynamic deformations of thick functionally graded elastic plates by using higher-order shear and normal deformable plate theory and meshless local Petrov-Galerkin method, *Composites, Part B: Engineering*, **35**, 685-697

25. Shariyat M., Jafari R., 2013, Nonlinear low-velocity impact response analysis of a radially preloaded two-directional-functionally graded circular plate: a refined contact stiffness approach, *Composites, Part B: Engineering*, **45**, 981-994

26. Shariyat M., Farzan F., 2013, Nonlinear eccentric low-velocity impact analysis of a highly prestressed FGM rectangular plate, using a refined contact law, *Archive of Applied Mechanics*, **83**, 623-641

27. Sun Dan., Luo S.N., 2011, The wave propagation and dynamic response of rectangular functionally graded material plates with completed clamped supports under impulse load, *European Journal of Mechanics – A/Solids*, **30**, 396-408

28. Swanson S.R., 2005, Contact deformation and stress in orthotropic plates, *Composites A*, **36**, 1421-1429

29. Turner J.R., 1980, Contact on a transversely isotropic half-space, or between two transversely isotropic bodies, *International Journal of Solids and Structures*, **16**, 409-419

30. Wirowski A., 2009, Free vibrations of thin annular plates made from functionally graded material, *Proceedings in Applied Mathematics and Mechanics*, **9**, 261-262

31. Wirowski A., 2011, Different methods of modelling vibrations of plates made of functionally graded materials, *Electronic Journal of Polish Agricultural Universities*, **14**, 3

32. Wirowski A., 2012, Self-vibration of thin plate band with non-linear functionally graded material, *Archives of Mechanics*, **64**, 603-615

33. Yaghoobi H., Torabi M., 2013, An analytical approach to large amplitude vibration and post--buckling of functionally graded beams rest on non-linear elastic foundation, *Journal of Theoretical and Applied Mechanics*, **51**, 39-52

34. Zhang Z., Paulino G.H., 2007, Wave propagation and dynamic analysis of smoothly graded heterogeneous continua using graded finite elements, *International Journal of Solids and Structures*, **44**, 3601-3626

35. Zienkiewicz O.C., Taylor R.L., 2005, *The Finite Element Method for Solid and Structural Mechanics*, Sixth Edition, Elsevier Butterworth-Heinemann, Oxford

Manuscript received July 31, 2014; accepted for print April 25, 2015